

A Kalman-Filter Method for Power Control in Broadband Wireless Networks

Kin K. Leung
AT&T Labs, Room 4-120
100 Schulz Drive
Red Bank, NJ 07701
Email: kkleung@research.att.com

Abstract: A Kalman-filter method for power control is proposed for broadband, packet-switched TDMA wireless networks. By observing the temporal correlation of co-channel interference when transmitters can send data contiguously, a Kalman filter is used to predict interference power in the future. Based on the predicted interference and estimated path gain between the transmitter and receiver, transmission power is determined to achieve a desired signal-to-interference-plus-noise ratio (SINR).

Performance results reveal that the Kalman-filter method for power control provides a significant performance improvement. Specifically, when a message consists of 10 packets on average, the 90 and 95 percentile of the SINR by the new method are 3.94 and 5.53 dB above those when no power control is in use, and lie just 0.73 and 1.04dB below the upper-bound performance of the optimal power control, respectively, in a system with 4-sector cells and an interleaved frequency assignment of a reuse factor of 2/8 [WL98]. As a by-product, these results show that the cell layout and assignment scheme combined with the new method for power control can be used to support high-speed data services.

1. INTRODUCTION

There is a growing demand for broadband wireless networks as work-at-home, telecommuting and Internet access have become very popular. High-speed packet services are needed to provide: a) efficient access to World Wide Web for information and entertainment on the Internet, b) remote access for telecommuters to their computer and data at the office, and c) multimedia services such as voice, image and video. Given the proliferation of Internet Protocol (IP) networks, it is important to consider and design broadband wireless networks that support IP. Towards this goal, it is natural to allow terminals and base stations to send data in multiple packets contiguously on a "connectionless" basis.

Dynamic transmission power control has been widely studied and practiced to combat and manage interference in cellular radio networks; see e.g., [Z92a], [FM93], [EKBNS96] and [RZ98]. Specifically, power control has been shown to be a useful technique to improve performance and capacity of time-division-multiple-access (TDMA) wireless networks. In addition to performance improvement, power control is actually essential in solving the near-far problem so that the base station can receive the

same power level from various transmitting terminals in code-division-multiple-access (CDMA) networks [AC93], [AC94], [EKBNS96]. In this paper, we focus on broadband, packet-switched TDMA networks with user data rates up to several megabits per second, link lengths (or cell size) typically less than 10 kilometers and operating frequency in the range of 1 to 5 GHz.

Existing power control algorithms for wireless networks can be categorized into two classes: *signal-based* and *signal-to-interference-ratio (SIR) based* power control. Signal-based power control [W93] [HWJ97] adjusts the transmission power based on the received signal strength, which in turn depends on path loss, shadowing and fading of the radio link between the transmitter and receiver. In contrast, SIR-based control [Z92a], [Z92b], [FM93], [GVG94] changes the power according to the ratio of signal and co-channel interference (possibly plus noise) power levels. (Since only co-channel interference is considered here, it is simply referred to as *interference* in the following.) It has been shown that SIR-based power control outperforms signal-based control, although the former is more complicated in implementation.

To the best of our knowledge, power control algorithms in the literature are proposed explicitly or implicitly for circuit-switched networks. Many of them such as [Z92b], [FM93], [GVGZ93], [GVG94] and [UY98] are iterative algorithms that require re-adjustments of transmission power over the entire call duration. As a result, such algorithms are applicable mainly to calls with relatively long holding time. For the same reason, they cannot be applied directly to packet-switching networks due to the burstiness of data packets, coupled with irregular transmission schedule in these networks. Therefore, there is a need to devise an appropriate power control algorithm for broadband, packet-switched TDMA networks, and this is the topic of this paper.

2. MOTIVATION FOR NEW POWER CONTROL

To help illustrate our ideas for wireless IP networks, let us assume that time is divided into *slots*, and the slot size is appropriately chosen to support the applications, while controlling the protocol overhead to achieve efficient radio bandwidth usage. Let each data message be divided into a number of packets, each of which can be transmitted in one time slot. As in typical IP networks, the message length (in terms of the number of packets or equivalently

time slots) varies randomly from message to message. Despite such randomness, the networks allow multiple, contiguous time slots to be used by the same terminal or base station for transmitting a message. As a consequence, the interference at a given receiver is correlated from one time slot to the next. We observe that such *temporal correlation* for the interference becomes strong quickly when the message length increases from one. For this reason, based on the interference measurements in previous slots, one can apply appropriate methods to predict the interference power to be received at a terminal or base station in the next time slot. Based on the predicted interference and estimated path gain between the transmitter and receiver, the transmission power in the next time slot can be determined to achieve the desired performance in terms of *signal-to-interference-plus-noise ratio* (SINR). These are the key ideas behind the power control algorithm proposed in the following.

In particular, we propose to use a Kalman filter [BH97] [H96] to predict the interference power, thus our power control algorithm is referred to as the *Kalman-filter method*. The advantage of the Kalman filter is that it is simple due to its recursive structure and robust over a wide range of parameters and conditions, and possibly provides an optimal estimate with minimum mean square error. It is well known that Kalman filter has been applied successfully to many systems [BH97]. As for wireless network applications, [DJM96] proposes using a Kalman filter for call admission in CDMA networks. We report here that Kalman filtering is also useful in controlling transmission power in TDMA networks.

To understand why power control can be crucial in the design of broadband TDMA networks, especially for low frequency reuse factor, let us consider a 4-sector cellular system with the (static) *interleaved channel assignment* (ICA) proposed in [WL98], as shown in Figure 1. In this layout, each cell is divided into four sectors and each sector is served by a 60° antenna. In the ICA scheme, each cell in the same column is assigned four channels (or channel sets), one for each of its four sectors. To take full advantage of the directivity of sectoral antennas, the channels assigned to the corresponding sectors of adjacent cells in the same column are interleaved. For example, channel 1 and 2 are assigned to the upper-left sectors in the middle column of cells in Figure 1 in an interleaved fashion; these channels are assigned the upper-right sectors of the cells in the same way. Similarly, channel 3 and 4 are assigned to the lower-left and lower-right sectors interleavingly in the same cell column. The assignment in this figure allows cells in a neighboring column to use a different set of four channels, thus the assignment yields a frequency reuse factor of $2/8$ (i.e., a channel is reused in every two cells and in every eight sectors). Using simulation techniques with reasonable assumptions and typical radio parameters (see Section 5 for details), Table 1 presents SINR percentiles for the uplink under various power control schemes in the system in Figure 1. Note that full power control adjusts the transmission power to fully compensate for the path loss and shadow fading from

a terminal to its base station, while the optimal power control (without considering thermal noise) is the method by [GVG94], which maximizes the minimum SIR among all links by balancing the transmission power. As shown in the table, comparing with no power control, a performance improvement of as much as 10dB can be achieved when the optimal control is employed. This large potential performance gain has motivated us to devise an appropriate power control scheme with a hope of achieving performance as close to the optimal as possible.

The organization of the rest of this paper is as follows. In section 3, the Kalman-filter method for power control is presented. The theoretical basis of the new method is discussed in Section 4. Then, in Section 5, we use simulation techniques to study the performance of the new method for the system shown in Figure 1. In addition, we also explain and interpret the numerical results. Finally, we present our conclusions and future work in Section 6.

3. A KALMAN-FILTER METHOD FOR POWER CONTROL

Although the Kalman-filter method for power control is applicable to both uplink (from terminal to base station) and downlink (from base station to terminal), our discussion will focus on the uplink here.

3.1 System Assumptions

1. Given that a terminal and its base station communicate directly with each other, we assume that the path gain between them (e.g., the sum of the path loss and shadow fading for the radio link) can be estimated accurately by measurements. This is a reasonable assumption, especially for the link quality not changing much in time when the terminal is moving at a very slow speed or stationary.
2. The multi-access control (MAC) protocol in use allows at most one terminal in each sector or cell to send data at a time; that is, no data contention occurs within the same sector or cell. In addition, the base station knows which terminal is scheduled to transmit at different times. (Both requirements can be achieved by using, for example, polling schemes as the MAC protocol. Having data contention in the same sector or cell will further complicate the power control problem as the interference power fluctuates even more, depending on whether or not more than one terminals transmit concurrently in a sector or cell.) When a terminal is permitted to transmit, it can send packets in multiple time slots contiguously.
3. Due to large volume of data involved, base stations cannot exchange information among themselves on a per packet basis in real time. Thus, it is extremely difficult to estimate how much interference one transmission causes to others in neighboring cells.
4. Interference power in each time slot can be measured quickly but possibly with noise and errors at each base station. At a high level, the interference power is equal to the difference between the total

received power and the power of the desired signal, where the latter can be measured by filtering based on the training symbols for the signal. In fact, such measurements can be involved and challenging, especially when time duration is short; see e.g., [AS95], [AMY96] and [A97].

3.2 Interference Prediction by Kalman Filter

As mentioned above, despite of the burstiness of packet traffic, interference is correlated in time in wireless IP networks. This temporal correlation enables us to employ a Kalman filter to predict the amount of interference to be received at a base station in the immediate future.

Let I_n be the actual interference-plus-noise power in dBm received in time slot n at a given base station. In other words, I_n is the "process state" to be estimated by the Kalman filter. We assume that the noise power, which depends on the channel bandwidth, is given and fixed. For brevity, unless stated otherwise, the interference plus thermal noise is simply referred to as *interference* in the following. The dynamics of the interference power is described by

$$I_n = I_{n-1} + F_n \quad (1)$$

where F_n represents the fluctuation of interference power for slot n as terminals may start new transmissions and/or adjust their transmission power in the time slot. In the terminology of Kalman filter, F_n is the "process noise." Let Z_n be the measured interference power in slot n . Then,

$$Z_n = I_n + E_n \quad (2)$$

where E_n is the "measurement noise." Eq.(1) and (2) are commonly referred to as the *signal generation model*. By the Kalman filter theory [BH97], the time and measurement update equations for the interference power are:

$$\tilde{I}_{n+1} = \hat{I}_n \quad (3)$$

$$\tilde{P}_{n+1} = \hat{P}_n + Q_n \quad (4)$$

$$K_n = \tilde{P}_n(\tilde{P}_n + R_n)^{-1} \quad (5)$$

$$\hat{I}_n = \tilde{I}_n + K_n(Z_n - \tilde{I}_n) \quad (6)$$

$$\hat{P}_n = (1 - K_n)\tilde{P}_n \quad (7)$$

where \tilde{I}_n and \hat{I}_n are the a priori and a posteriori estimate of I_n , \tilde{P}_n and \hat{P}_n are the a priori and a posteriori estimate error variance, K_n is the Kalman gain, and Q_n and R_n are the variance for the process noise F_n and measurement noise E_n , respectively.

Clearly, Q_n and R_n need to be estimated appropriately as input to (4) and (5). For that purpose, we propose the following estimations based on the interference measurements in a sliding window of the last W slots:

$$\bar{Z}_n = \frac{1}{W} \sum_{i=n-W+1}^n Z_i \quad (8)$$

$$Q_n = \frac{1}{W-1} \sum_{i=n-W+1}^n [Z_i - \bar{Z}_n]^2 \quad (9)$$

$$R_n = \eta Q_n \quad (10)$$

where η is a constant between 0 and 1. Strictly speaking, Q_n in (9) is an estimate of the variance of the sum of the process and measurement noise because measurements Z_n 's include the fluctuation of both interference and measurement errors. However, since the standard deviation of the interference power can reach as much as tens of decibels, which is much higher than typical measurement errors, (9) yields a good variance estimation for the process noise F_n . In addition, the choice of R_n according to (10) with η less than 1 is reasonable because the measurement noise (error) is likely to be proportional to, but smaller than, the fluctuation of interference power. Furthermore, the sliding window size W should be at least several times the average message length so that multiple terminals are likely to have transmitted during the time window, thus capturing changes of interference power.

It is noteworthy that the process noise F_n in (1) does not have a normal distribution, a requirement for the Kalman filter to minimize the mean square error. However, in special cases when thermal noise is not considered and the interference fluctuation is dominated by shadow fading, which is known to have lognormal distributions [R96], F_n in dBm is indeed normally distributed. For example, such domination by shadow fading can occur for static channel assignments with high frequency reuse factor. In this case, cochannel cells are far away from the target cell such that the path loss from various transmitting terminals in the same cochannel cell to the target cell very much remains constant. Thus, the fluctuation of F_n is mainly determined by the shadow fading between the transmitting terminal in the co-channel cell and the receiving base station in the target cell. Although F_n is not normally distributed in general, especially for frequency assignments with low reuse factors, our results show that the Kalman filter gives excellent interference predictions when a message consists of more than several packets on average.

For each slot n , the interference measurements are input to (9) and (10) to estimate Q_n and R_n . Using these values and the current measurement, (5) to (7) yield the Kalman gain, and the a posteriori estimates for I_n and P_n , respectively. The a priori estimates for the next time slot are given by (3) and (4). In particular, \tilde{I}_{n+1} in (3) is used as the predicted interference power in slot $n+1$ for power control as follows.

3.3 Determination of Transmission Power

Let us begin with some notation. Let β^* be the target SINR, p_n the transmission power and g_n the path gain from the transmitting terminal to the base station for slot n , respectively. While I_n and \tilde{I}_n represent the actual and estimated interference power in dBm, we use i_n and \tilde{i}_n to denote the respective values in the linear scale. By Assumption 1, the base station can measure and estimate g_n accurately. Based on this and the predicted interference

\tilde{I}_n in (3), the base station instructs (via a downlink channel) the terminal to transmit in slot n with power

$$p_n = \beta^* \frac{\tilde{i}_n}{g_n}. \quad (11)$$

The goal of this setting of transmission power is to choose just enough power to achieve the target SINR β^* , thus minimizing interference to others without degrading one's link quality. In fact, different SINR targets can be used in (11) for different terminals, depending on their path gain to the associated base stations and their application needs. For example, for a poor radio link with large path loss and unfavorable shadowing, the link can adapt to the poor quality by using a smaller size of modulation constellation. Thus, a lower SINR target is used in (11) to support a decreased data rate for the terminal. Nevertheless, we assume all terminals have an identical target SINR here.

When power is selected according to (11), the actual SINR β_n received at the base station in slot n is given by

$$\beta_n = \frac{p_n g_n}{i_n} = \beta^* \frac{\tilde{i}_n}{i_n} \quad (12)$$

where i_n is the actual interference power in mW for slot n . It is clear from (12) that when the interference prediction by the Kalman filter is accurate (i.e., $\tilde{i}_n \approx i_n$), the target SINR is achieved. Even when \tilde{i}_n does not predict i_n exactly, the method also helps in reducing the spread of β_n , provided that \tilde{i}_n and i_n are strongly correlated. In fact, the way that (11) selects the transmission power tends to enhance the correlation between \tilde{i}_n and i_n . This is so because a higher predicted interference \tilde{i}_n yields a higher transmission power p_n , which in turn causes the actual interference i_n to be higher.

3.4 Steps for the Kalman-Filter Method

The Kalman-filter method for controlling transmission power for each time slot n can be summarized as:

- a. For each time slot n , each base station measures the interference power for the time slot.
- b. The interference measurements are used as input to the Kalman filter in (3) to (10) to predict the interference power \tilde{I}_{n+1} (or equivalently, \tilde{i}_{n+1}) in the next slot $n+1$.
- c. Based on the MAC protocol in use (which satisfies Assumption 2), the base station tracks the path gain g_{n+1} , and selects the transmission power by (11) to meet a given target SINR for the terminal that transmits in slot $n+1$.
- d. The power level p_{n+1} is forwarded via the downlink to the terminal for actual transmission.

4. THEORETICAL BASIS FOR THE KALMAN-FILTER METHOD

The Kalman-filter method for power control is based on the theory of Foschini-Miljanic approach for power control [FM93], as explained as follows. Using our

notation, (13a) in [FM93] for adjusting transmission power can be re-written as

$$p_{n+1} = (1-\gamma)p_n + \gamma\beta^* \frac{z_n}{g_n} \quad (13)$$

where γ is a proportionality constant between 0 and 1, and z_n is the measured interference power in mW, corresponding to Z_n in dBm in (2). Evidently, γ provides "smoothing" effects as it tends to reduce changes of transmission power from one slot to the next. Results in [FM93] reveal that setting γ to 1 maximizes the convergence rate, which is needed for bursty packet traffic in the broadband wireless networks under consideration. However, it will be inappropriate to determine transmission power in the networks according to (13) when $\gamma=1$. This is so because, as discussed earlier, the interference power i_n (thus its measured value z_n) fluctuates greatly in the packet-switched networks, as different terminals are transmitting bursts of packets at times. Having observed the temporal correlation for the interference when a message consists of multiple packets, the Kalman-filter method bases on the previous interference measurements to predict interference power in the next time slot. Then, the power is determined by the predicted interference level according to (11). Clearly, (11) and (13) are similar. In fact, we can show the following:

Proposition. If the path gain (i.e., the combined effect of path loss and shadowing) and thermal noise for each radio link between a terminal and a base station does not change in time and the message length is infinitely long, the Kalman-filter method is identical to the Foschini-Miljanic approach with $\gamma=1$.

Proof. Since the path loss, shadow fading and noise for each radio link are assumed to remain unchanged in time and since a fixed set of terminals have been transmitting for an infinitely long time, we have a) $g_n = g_{n+1}$ for all n and b) the interference power received at a base station becomes a constant. The latter implies $Z_i \rightarrow \bar{Z}_n$ as $n \rightarrow \infty$ according to (8). Thus, both Q_n and R_n in (9) and (10) become zero. These zero values reveal that the Kalman gain K_n is 1 in (5). In turn, $\tilde{I}_n = Z_n$ by (6). Then, the filter predicts $\tilde{I}_{n+1} = \tilde{I}_n = Z_n$. Combining this with the fact a), the methods thus adjust the power in the same way as (11) and (13) with $\gamma=1$ become identical. \square

Due to terminal movement, change of thermal noise and fast fading (not considered in this paper), the path gain for a radio link always changes in time and message length may be short and bursty in the broadband, packet-switched networks. Nevertheless, the proposition helps understand that the Kalman-filter method and the Foschini-Miljanic approach indeed operate based on a similar theoretical basis. In particular, our performance results show that the Kalman-filter method is capable of providing significant improvement in term of SINR performance for finite message length over systems with no power control. More specifically, for typical radio environments, the Kalman-

filter method yields observable improvement even when a message consists of a few packets on average. These results are discussed as follows.

5. PERFORMANCE STUDY

Given the complexity of the system and control method, we choose to use simulation techniques to study the effectiveness of the Kalman-filter method. In the following, we first present the details of the simulation model and then discuss the performance results.

5.1 Simulation Model

We simulate the cell layout and interleaved channel assignment (ICA) [WL98] in Figure 1. A total of 19 cells are simulated. Each cell is divided into 4 sectors, each of which is served by a base station antenna located at the center of the cell. The beamwidth of each base station antenna is 60° , while terminals have omni-directional antennas. The radiation pattern for the base station antenna is assumed to be a parabolic shape; that is, a 3dB drop occurs at the beamwidth half angle and any direction beyond a threshold angle in clockwise or anti-clockwise direction suffers a given, fixed attenuation relative to the gain at the front direction, which is called the *front-to-back* (FTB) ratio. Thus, given the beamwidth and the FTB ratio, the parabolic-shape antenna pattern can be fully specified. For the 60° base station antenna with 20dB FTB ratio, this pattern yields a 3dB drop at the 30° angle in clockwise or anti-clockwise direction from the front direction, the threshold angle is 77.5° and the antenna gain at the front direction is 9.5dBi. The ICA (static) scheme in Figure 1 is considered where the frequency reuse factor is $2/8$ (i.e., reuse in every 2 cells or 8 sectors).

Each radio link between a terminal and its base station is characterized by a path-loss model with an exponent of 4 [R96] and lognormal shadow fading with a standard deviation of 8dB. Fast fading is not considered in this study. Cell radius is assumed to be 1 Km and the path loss at 100m from the cell center is -70dB. Thermal noise power is fixed and equal to -115dBm (to approximate a use of 1MHz channel bandwidth).

To fully consider the effects of shadow fading and the antenna pattern, terminals are first placed randomly at $\pm 67.5^\circ$ from the front direction of the base station antenna and as much as 1.25 times the cell radius from the center of each cell. Then, each terminal selects the base station that provides the strongest signal power. The process is repeated until each sector serves 500 terminals. To provide accurate results, only statistics in the middle cell in Figure 1 are collected and reported below. In addition, each simulation is repeated with 5 different sets of random seeds (e.g., for populating terminals and selecting shadow fading) to ensure correctness and results presented below are aggregated results of all five sets.

Message length is assumed to have a discrete form of Pareto distribution. We use a Pareto distribution because it has been shown to be appropriate for modeling IP traffic [WTSW97] and used by [U97] and [CS97] to study

wireless network performance. More precisely, each time a terminal transmits a message, the number of i slots (packets) used in the message transmission is characterized by the following cumulative distribution function:

$$H_i = 1 - \left[\frac{k}{i} \right]^\alpha \quad \text{for } i \geq k \in \mathbb{Z}^+ \text{ and } \alpha > 1. \quad (14)$$

where k and α are given parameters. Then, the probability that an arbitrary message consists of i packets is given by

$$h_i = \left[\frac{k}{i} \right]^\alpha - \left[\frac{k}{i+1} \right]^\alpha \quad \text{for } i \geq k \in \mathbb{Z}^+. \quad (15)$$

After some algebra, the average message length is

$$L = k + \sum_{i=k+1}^{\infty} \left[\frac{k}{i} \right]^\alpha. \quad (16)$$

It is known that the Pareto distribution has an infinite variance if $\alpha \leq 2$. Infinite variance should be avoided, otherwise our simulation model cannot reach a steady state and results may not have statistical significance. Thus, to guarantee finite variance, for a given L , we set $k = \lceil \frac{L}{2} \rceil$ to ensure $\alpha > 2$ where $\lceil y \rceil$ is the smallest integer greater than or equal to y . Using this k value, α can be solved from (16) to match the given average message length L .

Two adjustable parameters W and η for (9) and (10) are set to be 30 and 0.5, respectively. As discussed earlier, $W=30$ is appropriate as $L \leq 10$ in our study, whereas $\eta=0.5$ is appropriate because if η is too small, the Kalman gain K_n 's by (5) will be very close to 1, thus making the predicted interference level too close to the last measurement. Our numerical experiments reveal that the Kalman-filter method gives similar results for $W=50, 80$ and η ranging from 0.25 to 1.

For convenience, our simulation model assumes that terminals in all cells are synchronized at the slot boundary for transmission. (This assumption can be relaxed in practice with some minor performance degradation.) Furthermore, we assume 100% traffic load in this study. That is, there are always terminals ready for transmission in co-channel sectors. Thus, after a terminal transmits a message with a random length according to (14), the base station immediately schedules another randomly chosen terminal in the same sector to start a new transmission in the next time slot. To help us study the dynamic range for the power control schemes, the model assumes no limit on the actual transmission power.

Unless stated otherwise, the model also assumes that interference power in one time slot can be measured and used to determine the transmission power for the next slot. Nevertheless, a study of performance impacts due to delay in providing the transmission power to the transmitting terminal is also reported in the following.

5.2 Performance Results and Discussions

Figure 2 compares the SINR performance for the Kalman-filter method with that for no, full and optimal

power control. For no power control, transmission power is fixed at 30dBm, while the full power control scheme fully compensates for the path gain between a terminal and its base station (i.e., the combined path loss and shadow fading) such that the received signal strength at the base station is maintained at a fixed level of -80dBm.

Note that results in Table 1 are identical to those in Figure 2 for the no, full and optimal power control schemes. Results for the optimal power control, shown by solid line in the figure, are obtained by the method in [GVG94] based on SIR without considering thermal noise. The method assumes precise knowledge of path gain for all combinations of terminals and base stations. By knowing the path-gain matrix for the transmitting terminals and receiving base stations, the iterative method is executed until convergence to determine the optimal transmission power for each time slot. The transmission power is scaled in each iteration to avoid numerical underflow and overflow. Therefore, these results represent the upper bounds for the actual SINR performance for the system in Figure 1.

As for the Kalman-filter method, we set the target SINR β^* to be 18dB in (11). As shown by the dashed lines in Figure 2, when the message length is 1, the high (e.g., 90 to 99) percentiles of the SINR for the Kalman-filter method are very close to those for the full and no power control scheme. However, the performance for the new method improves rapidly as the average message length L increases. In particular, for $L = 10$, the 90 and 95 percentile of the SINR are 3.94 and 5.53 dB above those for no power control, which represent very significant performance improvement, and lie just 0.73 and 1.04dB below the upper-bound performance of the optimal power control (see Table 1 for the precise values), respectively.

Such improvement can best be explained by examining (12). As L increases, the temporal correlation for interference becomes strong, and the interference power i_n predicted by the Kalman filter is close to the actual value, i_n , thus achieving the target SINR. The Kalman-filter method is expected to perform even closer to the optimum when L is increased further. As expected, we observe in Figure 2 that the probability for SINR exceeding 18dB, the target SINR, for the Kalman-filter method drops quickly. This implies that good radio links can transmit at a low power, thus further reducing the amount of interference for co-channel sectors. In addition to the results for Pareto-distributed message length in Figure 2, we also obtained similar results for geometric-distributed message length.

To put these results in prospective, typical SINR requirement for standard modulation and equalization schemes (e.g., QPSK and decision feedback equalizer) for satisfactory detection lies between 10 to 15dB. To avoid excessive retransmissions due to detection failure for a given automatic retransmission request (ARQ) algorithm in use, the 90 to 95 percentile for the SINR should exceed the requirement. For a wireless network with a data rate of 1Mbps, a time slot can be chosen to be 0.5 msec; that is, each packet contains 500 bits, which is comparable to the

length of a TCP/IP acknowledgement (e.g., in web browsing applications) or the size of an ATM cell when the IP is supported by the ATM transport network. With these parameters, the average message length is likely to be greater than 10 for applications such as telecommuting where text emails (let alone those with attachments) can easily contain more than 5,000 bits.

From this prospective, results in Figure 2 reveal that the cell layout and the ICA scheme with a reuse factor of 2/8 combined with the Kalman-filter method for power control are capable of providing high-speed data service.

For $L = 10$, Figure 3 illustrates how the SINR performance for the Kalman-filter method improves when the target SINR, β^* in (11), increases from 12 to 20dB. As the target increases, the performance becomes close to the optimum. However, as intuitively expected, there exists a certain maximum target for given channel assignment, cell layout and radio parameters, without increasing transmission power to infinity.

We note that determining the maximum achievable SINR target in the Kalman-filter method for a cellular setting is an open issue. When thermal noise is not considered and the path-gain elements are constant, [Z92a] has proven that the maximum achievable SIR is determined by the largest real eigenvalue of the path-gain matrix. However, the path-gain matrix for uplink transmission in packet-switched networks is a time-dependent, random matrix because different terminals transmit bursts of packets at times. Thus, one can see that finding the maximum achievable target for the Kalman-filter method is complicated.

For the system in Figure 1, we studied the issue by means of experiments. It is found that when the target SINR is greater than 20dB, the simulation simply did not reach a steady state and the transmission power was set to be extremely high. Coincidentally, we observe that the 50 percentile SIR (with no noise) for the optimal power control [GVG94] is 20.37dB. This leads us to suggest that one can use the 50 percentile SIR as the maximum achievable SINR target for the Kalman-filter method, if the system under consideration is interference limited.

In fact, we have to choose a target somewhat lower than this "true" maximum in order to keep transmission power at a reasonable level. To help understand this, for $L = 10$, Figure 4 shows the distribution of transmission power for selecting 15, 18 and 20dB as the target SINR. It is interesting to observe that although a target of 20dB is achievable, it however requires excessive transmission power. At the other extreme, for 15dB as the target SINR, terminals do not fully utilize their typical, maximum transmission power of 30dBm. From these results, a target SINR of 18dB can be supported in practice.

So far, we have assumed that interference power in one time slot can be measured and used to determine the transmission power for the next slot. This assumption can be reasonable for the following scenario. Suppose that the downlink and uplink are supported by frequency division

duplex (FDD) and the timing for the downlink lags behind that for the uplink by half of a time slot. Furthermore, interference power can be measured during the beginning part of a slot (say slot i) on the uplink and transmission power for the next slot can be calculated quickly such that at the beginning of slot i on the downlink, the base station can send the power level to the transmitting terminal for slot $i + 1$.

As expected, there will be delay in providing power levels to transmitting terminals in some systems. Figure 5 shows the performance degradation due to such delay. Specifically, our results reveal that for $L = 10$ and $\beta^* = 18\text{dB}$, when terminals transmit in a slot (say slot i) at a power level computed based on the previous interference measurements up to slot $i - 2$ (i.e., experiencing a delay of one slot), the 90 and 95 percentile for the SINR for the Kalman-filter method drop by 0.86 and 1.43dB, respectively, from those with no delay. Despite these small decreases, the Kalman-filter method for power control still improves the SINR performance significantly over that when no or full power control schemes are employed. As expected, the minor performance degradation vanishes when the average message length is higher than 10.

6. OTHER IMPLEMENTATION CONSIDERATIONS

We have assumed in Assumption 1 (Section 3.1) that, especially for low-speed and stationary terminals, the path gain for the signal strength (i.e., from a terminal to its associated base station) can be measured and estimated accurately by the base station. Similar to the prediction of interference power, one can apply another Kalman filter to estimate the signal path gains. This may be needed when the signal strength fluctuates greatly in time because of movement of the terminals and/or fading.

In this study, we assume that transmission power has infinite precision. However, to enable efficient implementation, the transmission power should be discretized into multiple (e.g., 2^i for $i = 1, 2, 3, \dots$) levels, according to the desired tradeoffs between performance and signaling protocol overhead. Furthermore, transmission power is determined and adjusted every time slot. An alternative to that is to use a fixed power level for transmission of the entire message. For example, this approach is suitable for using polling schemes as the MAC protocol, where the transmission power can be included in the polling message and the polled terminal simply transmits at that power level if it has data to send. (See e.g., [CCYC97] for other benefits of polling schemes in wireless networks.) This approach can reduce the signaling complexity and overhead, probably with a small reduction in the SINR performance.

7. CONCLUSIONS AND FUTURE WORK

The Kalman-filter method for power control has been proposed for broadband, packet-switched TDMA wireless networks. By observing the temporal correlation of co-

channel interference when transmitters can send data contiguously, the method uses a Kalman filter to predict interference power in the future. Based on the predicted interference and estimated path gain between the transmitter and receiver, transmission power is determined to achieve a desired SINR performance. The new method is based on the theory of the Foschini-Miljanic algorithm for power control [FM93], although the latter is not suitable for packet networks. The new technique is simple for implementation due to its recursive structure and is robust over a wide range of parameters.

Our performance results reveal that the Kalman-filter method for power control provides a significant performance improvement in wireless packet networks. Specifically, when messages consist of 10 packets on average, the 90 and 95 percentile of the SINR by the new method are 3.94 and 5.53 dB above those when no power control is in use, and lie just 0.73 and 1.04dB below the upper-bound performance of the optimal power control, respectively, in a system of 4-sector cells using the interleaved channel assignment (ICA) with a frequency reuse factor of 2/8 [WL98]. As a by-product, these results show that this layout and assignment scheme combined with the Kalman-filter method for power control, can be used to support high-speed data services.

For third generation wireless networks, network performance will depend on the design of dynamic channel assignment (DCA), traffic scheduling, power control, MAC, adaptive modulation and coding scheme for link adaptation. Often, these issues have been studied separately. As results reported above have shown, an appropriate algorithm for power control can provide significant improvements in SINR performance (and thus network capacity). With the proposed method for power control as a basis, we are in the process of developing and studying new designs to consider these issues jointly, with a goal of achieving high spectral efficiency and capacity in practical networks.

Acknowledgment. Thanks are due to Paul Henry for his suggestions and comments that helped identify errors in early results of this work. The author thanks Li-Chun Wang for pointing out several references and his discussion. Thanks are also due to Lek Ariyavitakul, Justin Chuang, Martin Clark, Mitch Cox, Larry Greenstein, Xiaoxin Qiu, N.K. Shankar, Jim Whitehead and Ward Whitt for their discussion and comments.

REFERENCES

- [A97] M. Andersin, "Real-Time Estimation of the Signal to Interference Ratio in Cellular Radio Systems," *Proc. of IEEE Veh. Tech. Conf.*, 1997, pp.1089-1093.
- [AC93] S. Ariyavitakul and L.F. Chang, "Signal and Interference Statistics of a CDMA System with Feedback Power Control," *IEEE Trans. on Commun.*, Vol.41, No.11, Nov. 1993, pp.1626-1634.
- [AC94] S. Ariyavitakul and L.F. Chang, "Signal and Interference Statistics of a CDMA System with Feedback Power Control - Part II," *IEEE Trans. on*

- Commun.*, Vol.42, No.2-4, Feb-April 1994, pp.597-605.
- [AMY96] M. Andersin, N.B. Mandayam and R.D. Yates, "Subspace Based Estimation of the Signal to Interference Ratio for TDMA Cellular Systems," *Proc. of IEEE Veh. Tech. Conf.*, Atlanta, Georgia, April 1996, pp.742-748; also in *Wireless Networks*, Vol.4, 1998, pp.241-247.
- [AS95] M.D. Austin and G.L. Stüber, "In-Service Signal Quality Estimation for TDMA Cellular Systems," *Wireless Personal Communications*, Vol.2, No.3, 1995, pp.245-254.
- [BH97] R.G. Brown and P.Y.C. Hwang, *Introduction to Random Signals and Applied Kalman Filtering*, 3rd Edition, John Wiley & Sons, New York (1997).
- [CCYC97] C.S. Chang, K.C. Chen, M.Y. You and J.F. Chang, "Guaranteed Quality-of-Service Wireless Access to ATM Networks," *IEEE J. on Select. Areas in Commun.*, Vol.15, No.1, Jan. 1997, pp.106-118.
- [CS97] J.C. Chuang and N.R. Sollenberger, "Dynamic Packet Assignment for Advanced Cellular Internet Service," *Proc. IEEE Globecom'97*, Phoenix, AZ, Nov. 1997, pp.1596-1600.
- [DJM96] Z. Dziong, M. Jia and P. Mermelstein, "Adaptive Traffic Admission for Integrated Services in CDMA Wireless-Access Networks," *IEEE J. on Select. Areas in Commun.*, Vol.14, No.9, Dec. 1996, pp.1737-1747.
- [EKBNS96] Special issue on CDMA Networks, *IEEE J. on Select. Areas in Commun.*, Vol.14, No.9, Dec. 1996, A.K. Elhakeem, R. Kohno, P.W. Baier, M. Nakagawa, and D.L. Schilling (Ed.).
- [FM93] G.J. Foschini and Z. Miljanic, "A Simple Distributed Autonomous Power Control Algorithm and its Convergence," *IEEE Trans. on Veh. Tech.*, Vol.42, No.4, Nov. 1993, pp.641-646.
- [GVG94] S.A. Grandhi, R. Vijayan and D.J. Goodman, "Distributed Power Control in Cellular Radio Systems," *IEEE Trans. on Commun.*, Vol.42, No.2-4, Feb-April 1994, pp.226-228.
- [GVGZ93] S.A. Grandhi, R. Vijayan, D.J. Goodman and J. Zander, "Centralized Power Control in Cellular Radio Systems," *IEEE Trans. on Veh. Tech.*, Vol.42, No.4, Nov. 1993, pp.466-468.
- [H96] S. Haykin, *Adaptive Filter Theory*, 3rd Edition, Prentice Hall, New Jersey (1996).
- [HWJ97] Z.J. Haas, J.H. Winters and D.S. Johnson, "Simulation Results of the Capacity of Cellular Systems," *IEEE Trans. on Veh. Tech.*, Vol.46, No.4, Nov. 1997, pp.805-817.
- [R96] T.S. Rappaport, *Wireless Communications: Principles and Practice*, New York: IEEE Press and Prentice Hall, 1996.
- [RZ98] Special issue on power control, *Wireless Networks* 4 (1998) 3, Zvi Rosberg and Jens Zander (Ed.).
- [U97] UMTS 30.03 V3.0.0 (1997-05) Technical Report: Universal Mobile Telecommunications System (UMTS); Selection procedures for the choice of radio transmission technologies of the UMTS (UMTS 30.03 version 3.0.0).
- [UY98] S. Ulukus and R.D. Yates, "Stochastic Power Control for Cellular Radio Systems," *IEEE Trans. on Commun.*, Vol.46, No.6, June 1998, pp.784-798.
- [W93] J.F. Whitehead, "Signal-level-based Dynamic Power Control for Co-channel Interference Management," *Proc. of IEEE Veh. Tech. Conf.*, Secaucus, NJ, May 1993, pp.499-502.
- [WL98] L.C. Wang and K.K. Leung, "A High-Capacity Cellular Network by Improved Sectorization and Interleaved Channel Assignment," *Multiaaccess, Mobility and Teletraffic for Wireless Communications: Vol.3* (MMT'98), K. Leung and B. Vojcic (Ed.), Kluwer Academic Publishers, Boston (1999), pp.43-58.
- [WTSW97] W. Willinger, M. Taqqu, R. Sherman and D. Wilson, "Self-Similarity Through High-Variability: Statistical Analysis of Ethernet LAN Traffic at the Source Level," *IEEE/ACM Trans. on Networking*, Vol.5, No.1, Feb. 1997, pp.71-86.
- [Z92a] J. Zander, "Performance of Optimum Transmitter Power Control in Cellular Radio Systems," *IEEE Trans. on Veh. Tech.*, Vol.41, No.1, Feb. 1992, pp.57-62.
- [Z92b] J. Zander, "Distributed Cochannel Interference Control in Cellular Radio Systems," *IEEE Trans. on Veh. Tech.*, Vol.41, No.3, Aug. 1992, pp.305-311.

Fig.1. A 4-Sector Cell Layout and ICA

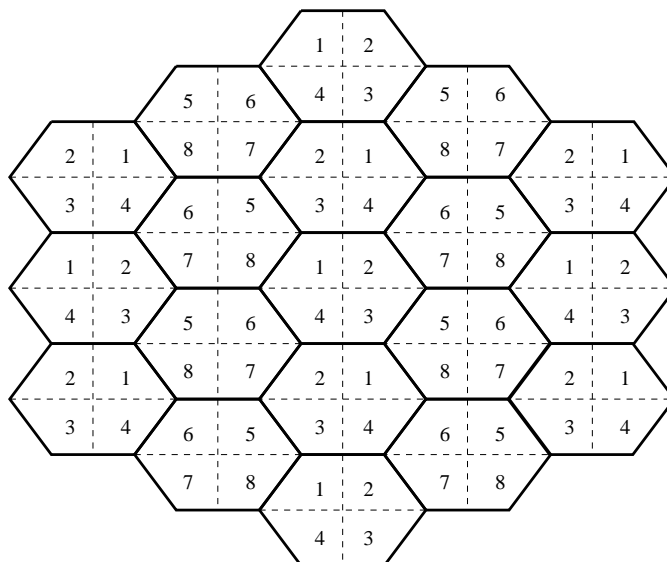


Table 1. SINR for the ICA with Reuse Factor 2/8.

Power control	SINR Percentile (dB)		
	90%	95%	99%
No	10.5748	7.2069	0.6229
Full	9.3661	6.3769	1.2396
Optimal	15.3082	13.8104	11.0144

Fig.2. Comparison of SINR Performance

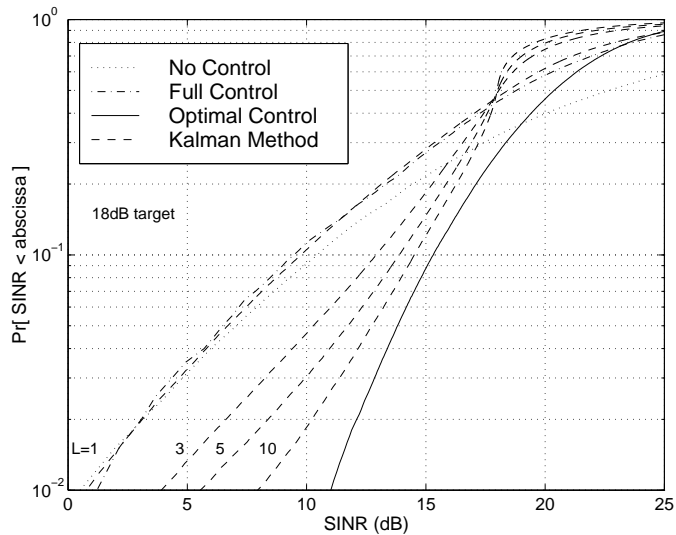


Fig.3. Performance Impacts of SINR Target

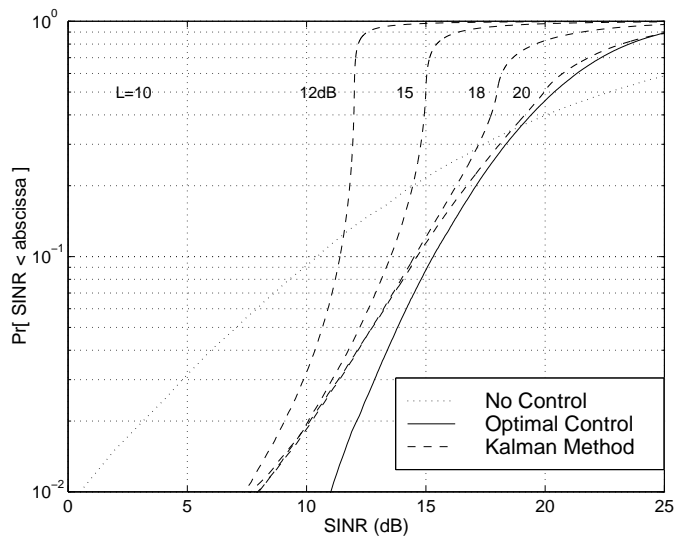


Fig.4. Transmission Power Distribution

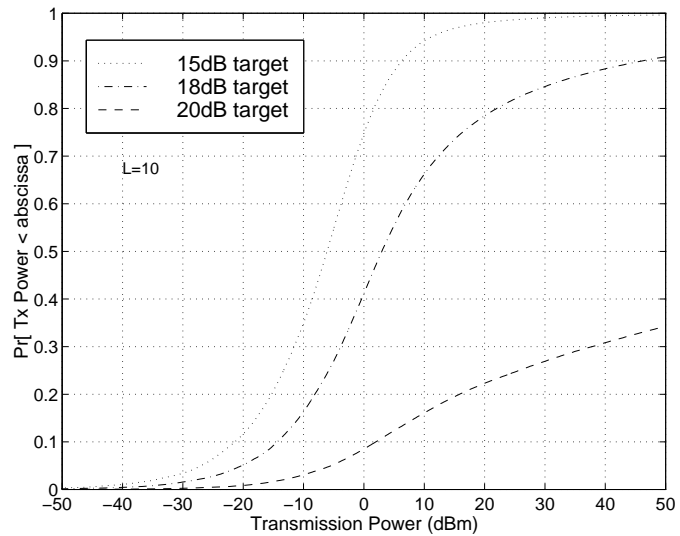


Fig.5. Performance Impacts of Feedback Delay

